ELSEVIER

Journal of Alloys and Compounds 466 (2008) 507–511

Journal of ALLOYS AND COMPOUNDS

www.elsevier.com/locate/jallcom

Effect of buffer layer thickness and epilayer growth temperature on crystalline quality of $InAs_{0.9}Sb_{0.1}$ grown by MOCVD

Shuzhen Yu [a,b], Guoqing Miao [a,*], Jianchun Xie [a], Yixin Jin [a], Tiemin Zhang [a,b], Hang Song [a], Hong Jiang [a], Zhiming Li [a]

[a] *Key Laboratory of Excited State Processes, Changchun Institute of Optics, Fine Mechanics and Physics, The Chinese Academy of Sciences, Changchun 130033, China*

[b] *Graduate School of the Chinese Academy of Sciences, Beijing 100049, China*

Received 19 September 2007; received in revised form 14 November 2007; accepted 21 November 2007
Available online 26 November 2007

Abstract

$InAs_{0.9}Sb_{0.1}$ epilayers are grown on GaAs (001) substrates by metal organic chemical vapor deposition (MOCVD). In order to relax compressive strain caused by lattice mismatch between $InAs_{0.9}Sb_{0.1}$ and GaAs, we employ a two-step growth method in which low temperature (430 °C) $InAs_{0.9}Sb_{0.1}$ buffer layers with different thicknesses are introduced into the structure. Effect of the buffer layer thickness and the epilayer's growth temperature on crystalline quality of the epilayer is investigated, respectively. It is clear that there are strip pyramids paralleling with each other on most surface of the samples. The crystalline quality gets well obviously when the buffer layer thickness change from 0 to 50 nm, but it gets worse when the buffer layer thickness increases to 100 nm. It is also shown that the crystalline quality of the epilayer is improved obviously when the epilayer is grown at 500 °C, and it gets worse when the growth temperature decreases or increases.

Keywords: $InAs_{0.9}Sb_{0.1}$; MOCVD; Two-step growth method

1. Introduction

InAsSb ternary alloys have received increasing attention due to their advantages of high device operation temperature, high stability, as well as high electron mobility [1–6] for their infrared applications. Such as InAsSb infrared photodetectors can operate at room temperature and they have small bandgap changes from compositional variations, more stable parameters with respect to external influences. The InAsSb ternary alloys are mismatched to GaAs by between 7.2% and 14.5%, depending on composition. So there exist compressive strains between epilayers and substrates which induce kinds of defects. The problem can be reduced by the incorporation of thin strained layers or by the growth of buffer layers with or without graded lattice parameters [6–9]. Supperlattice based on InAsSb are principally used as buffer layers. But a single step strain relaxation approach can simplify the growth procedure. Such as the two-step growth method which consists of an initial low temperature buffer layer and following a high temperature growth of epilayer has often been employed to grow high mismatch epilayers. The low temperature buffer layer is believed to act as a template for succeeding high temperature grown epilayers and to accommodate lattice strain caused by both lattice mismatch and thermal one. Two-step growth methods of SiGe [10], AlGaN [11], InAs [12] and GaN [13] have been reported. However, $InAs_{0.9}Sb_{0.1}$ with this growth method is rarely studied. In this paper, low temperature (430 °C) $InAs_{0.9}Sb_{0.1}$ buffer layers are employed in growing $InAs_{0.9}Sb_{0.1}$ epilayers on GaAs substrates. We utilize scanning electron microscopy (SEM), Raman scattering, photoluminescence (PL) and Hall measurement to study the effect of the buffer layer thickness and the epilayer's growth temperature on the crystalline quality of the epilayers.

2. Experimental

Experiments were carried out by MOCVD in a horizontal reactor operating at a low pressure of 10 kPa. Hydrogen was used as the carried gas at a total flow of 2.0 L/min. The sources of In, Sb and As were trimethylindium (TMIn), trimethylantimony (TMSb) and AsH_3 diluted to 10% in hydrogen,

* Corresponding author.
E-mail address: miaogq@ciomp.ac.cn (G. Miao).

0925-8388/$ – see front matter © 2007 Elsevier B.V. All rights reserved.
doi:10.1016/j.jallcom.2007.11.088

Table 1
Growth parameters for the eight samples

Sample number	Buffer layer thickness (nm)	Epilayer growth temperature (°C)
A1	10	520
A2	30	520
A3	50	520
A4	100	520
B1	30	480
B2	30	500
B3	30	520
B4	30	550

Samples A1, A2, A3 and A4 are grown with different buffer layer thicknesses. The difference between samples B1, B2, B3 and B4 is $InAs_{0.9}Sb_{0.1}$ epilayers' growth temperature.

respectively. After growing the $InAs_{0.9}Sb_{0.1}$ buffer layers at 430 °C, AsH_3 and TMSb were used as protecting atmosphere during raising temperature from 430 °C to the $InAs_{0.9}Sb_{0.1}$ epilayer's growth temperature. Then, TMIn was inputted again to grow the epilayers. The flow of TMIn, TMSb and AsH_3 were varied from 0.5×10^{-5} to 1.0×10^{-5}, 0.15×10^{-5} to 0.56×10^{-5} and 0.6×10^{-5} to 0.8×10^{-5} mol/min. The thickness of all the samples is 0.7 μm. Growth parameters for eight samples to be considered in this paper were summarized in Table 1. For samples A1, A2, A3 and A4, the buffer layers were grown at 430 °C and the epilayers were grown at 520 °C. Their buffer layer thicknesses were 10, 30, 50 and 100 nm, respectively. For samples B1, B2, B3 and B4, the 30-nm thick buffer layers were grown at 430 °C, and the epilayers were grown at 480, 500, 520 and 550 °C, respectively.

3. Results and discussion

Fig. 1 shows SEM of samples A1, A2, A3 and A4. The growth parameters such as the V/III ratios, the flow rates of TMIn, TMSb and AsH_3, the thicknesses of the epilayers and the reactor pressure are identical with each other during the four samples growth except for the $InAs_{0.9}Sb_{0.1}$ buffer layers thicknesses. As increasing the buffer layers thickness, surface morphologies with different number and size of paralleling strip pyramids can be visible. Sample A1 has a large number of small strip pyramids. Samples A2 and A3 have fewer strip pyramids, but their size became larger. For sample A4, there are not only some larger strip pyramids but also a lot of small strip pyramids on its surface. The energy-dispersed X-ray spectrometry (EDS) taken from the strip pyramids and from the smooth areas is almost the same. So the strip pyramids are not the separate elemental antimony or indium phase. Nakamura [7,14] thought the strip pyramids imply a different incorporation behavior of the atoms to the growth surface compared with other compositional $InAs_xSb_{1-x}$ ($x \leq 0.6$). Surface morphology of the $InAs_{0.9}Sb_{0.1}$ epilayers grown without buffer layers appears higher density of small paralleling strip pyramids (not shown here) which caused by compressive strains between epilayers and GaAs substrates. Due to large lattice mismatch, the buffer layers grown on GaAs substrates form islands in the initial growth stage. After the islands exceed a critical size, the compressive strain in the islands is relaxed by introduction of misfit dislocation. Most of the misfit dislocations exist

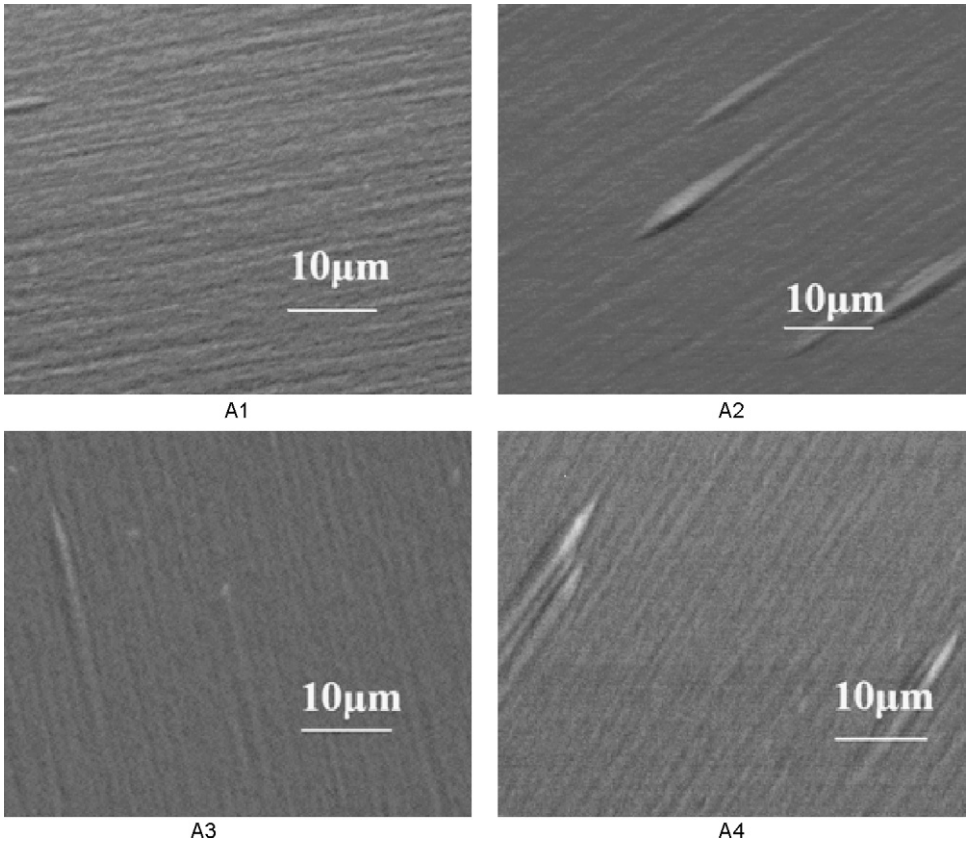

Fig. 1. SEM of samples A1, A2, A3 and A4. The buffer layer thickness of A1 is 10 nm, A2 is 30 nm, A3 is 50 nm, A4 is 100 nm.

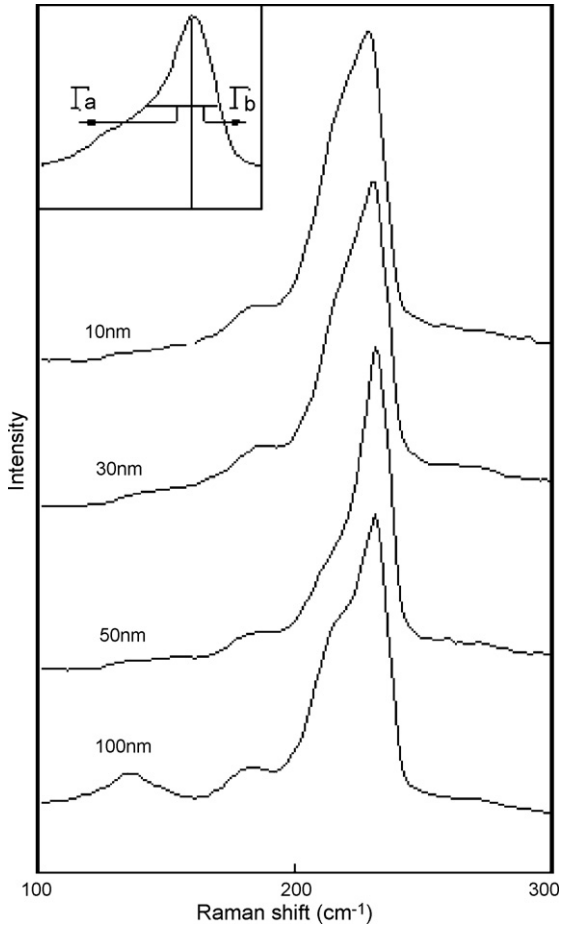

Fig. 2. Raman scattering spectra of the $InAs_{0.9}Sb_{0.1}$ epilayers for which buffer layer thicknesses are different. The inset shows Γ_a and Γ_b which is used in the asymmetry ratio (Γ_a/Γ_b) of Raman scattering spectra.

in the buffer layers, especially in the plane heterojunction, but the compressive strains do not relax completely. Those residual compressive strains still induce kinds of defects such as paralleling strip pyramids on the epilayer's surface and misfit dislocations in the epilayers. So, on the surface, the paralleling strip pyramids do not disappear and there are residual misfit dislocations in the epilayers. The relaxation of compressive strain is different with different buffer layer thicknesses. That is, there exists appropriate thickness of the buffer layers that can relax the compressive strain in maximum.

Raman scattering spectra for $InAs_{0.9}Sb_{0.1}$ epilayers with different buffer layer thicknesses are shown in Fig. 2. Two peaks can be visible which correspond to the InAs-like LO mode and the InSb-like LO mode. That is $InAs_{0.9}Sb_{0.1}$ epilayers grown on GaAs (0 0 1) substrates reveal two-mode behaviors that is identical with Li [15]. A shoulder lies between the InAs-like LO mode and the InSb-like LO mode for all the samples. This shoulder has been observed by Li [15] and Cherng [16] for InAsSb, by Kakimoto [17] for InGaAs, and was interpreted as being due to disorder-activated optical (DAO) phonons. For sample A4, a broadband with Raman shift 136 cm^{-1} is observed. A similar broadband which exists between 130 and 150 cm^{-1} has been reported by Cherng [16]. This band was identified as been due to

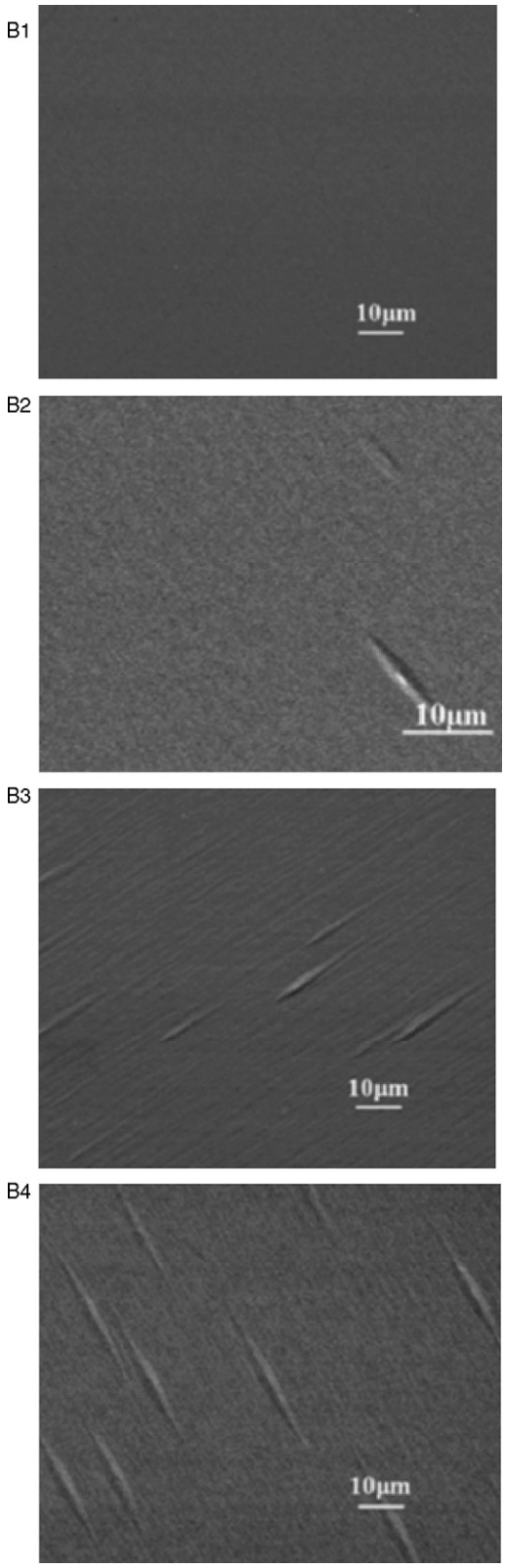

Fig. 3. SEM of samples B1, B2, B3 and B4. The $InAs_{0.9}Sb_{0.1}$ epilayers' growth temperature of B1 is 480 °C, B2 is 500 °C, B3 is 520 °C, B4 is 550 °C.

disorder-activated longitudinal acoustic (DALA) phonons [16]. Raman scattering is determined by the overlap integral of electrons, phonons and photons, the finite phonon mode will lead to the broadening and asymmetry of the Raman scattering line shape [18]. Therefore, the full-width at half-maximum (FWHM) and the asymmetry ratio (Γ_a/Γ_b) of Raman scattering spectra can determine the alloy disorder, consequently characterize the crystalline quality of samples. Γ_a and Γ_b are two half-widths at half-maximum of the Raman scattering peak which are shown in inset of Fig. 2. The FWHM and the Γ_a/Γ_b of Raman scattering spectra for samples A1, A2, A3 and A4 are 26.33, 23.82, 12.54, 27.58 cm^{-1} and 6.37, 4.68, 2.74, 5.57, respectively. It is obvious that sample A3 has the minimum FWHM and Γ_a/Γ_b. Considering the surface morphology, the FWHM and the Γ_a/Γ_b, the thickness of the buffer layer as thick as 50 nm is an effective thickness for improving the crystalline quality of the epilayers on GaAs (0 0 1) substrates.

Fig. 3 presents SEM of the samples B1, B2, B3 and B4. Only sample B1 does not have strip pyramids, because epilayers grown at low temperature (480 °C) can more effectively relax the residual compressive strain [21]. But electrical property of the epilayers becomes poor simultaneously [19]. The size and the number of the paralleling strip pyramids increase when the growth temperature of the epilayers is increased. Room temperature electron mobility of samples B1, B2, B3 and B4 are 3108, 3718, 3466 and 3299 cm^2/V s, respectively. It is clear that sample B2 has the highest electron mobility. In the epilayers, the residual misfit dislocations that act as scattering center reduce the carrier mobility [20,21]. Hereby, the density of misfit dislocations in the epilayer of sample B2 is the least. The 77 K photoluminescence spectra of the samples are shown in Fig. 4. The band gap energy of samples is about 0.325 eV that matches extremely well with the calculated value of 0.3257 eV [22]. The PL measurement was performed with the experimental system being purged with dry air, hence the carbon dioxide (CO_2) absorption at 0.291 eV can be detectable [23,24]. This coincides with the fact that the CO_2 absorption features at approximately 0.29 eV in the PL lines of samples B1, B3 are observed. For samples B2 and B4, the broadening of the PL lines cover up the CO_2 absorption signals. The Γ_a/Γ_b of Raman scattering spectrum and the FWHM of PL for samples B1, B2, B3 and B4 with different growth temperatures of the epilayers are plotted in Fig. 5. For sample B2, the Γ_a/Γ_b of Raman scattering spectrum is 2.39 and the FWHM of PL is 30.4 emV. Both are the minimum. In general, some defects such as misfit dislocations are known to broaden photoluminescence linewidths. So the change of the FWHM of PL is related to the growth temperatures of the epilayers. That is, sample B2 for which epilayers' growth temperature is 500 °C has the highest crystalline quality.

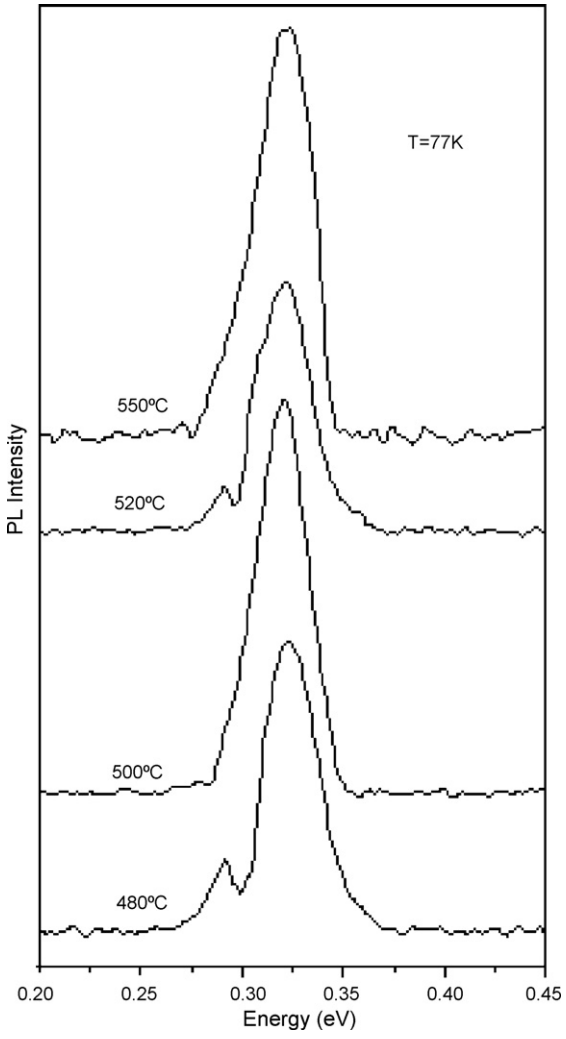

Fig. 4. The 77 K photoluminescence of samples B1, B2, B3 and B4. The excitation source is Ar-ion laser operating at 514.5 nm.

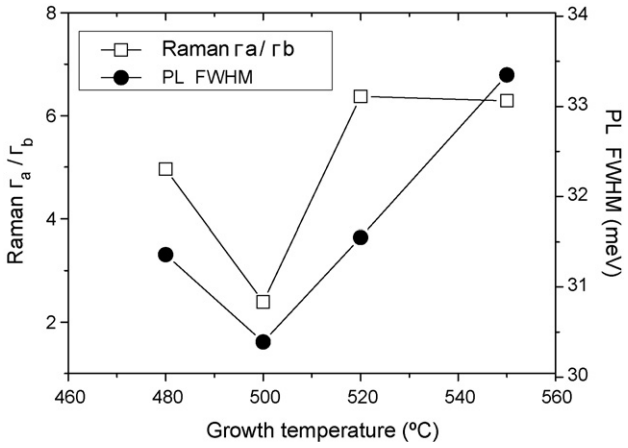

Fig. 5. The asymmetry ratio (Γ_a/Γ_b) of Raman scattering spectra and the FWHM of PL (77 K) for samples B1, B2, B3 and B4 with different growth temperatures of the $InAs_{0.9}Sb_{0.1}$ epilayers.

4. Conclusions

The $InAs_{0.9}Sb_{0.1}$ epilayers grown on GaAs (0 0 1) substrates were obtained by MOCVD with the two-step growth method. The surface morphologies of the samples are observed by SEM. It is clear that there are paralleling strip pyramids on most surface of the samples. The $InAs_{0.9}Sb_{0.1}$ buffer layers grown at 430 °C can effectively relax the compressive strains by the generation of a high density of misfit dislocations at the heterojunctions

between buffer layers and substrates. But there are residual compressive strains. Those residual compressive strains induce kinds of defects such as paralleling strip pyramids on the epilayers' surface and misfit dislocations in the epilayers. The crystalline quality of the samples is characterized using the FWHM and the Γ_a/Γ_b of Raman scattering spectra, the FWHM of PL (77 K) and the room temperature Hall measurement. It is found that the optimum thickness of the buffer layer is 50 nm and the optimum growth temperature of the epilayer is 500 °C.

Acknowledgements

This work is supported by Projects of National Natural Science Foundation of China under grant No. 50632060 and No. 50372067.

References

[1] C. Besikci, Y.H. Choi, G. Labeyrie, E. Bigan, M. Razeghi, J.B. Cohen, J. Carsello, V.P. Dravid, J. Appl. Phys. 76 (1994) 5820–5828.
[2] H.H. Gao, A. Krier, V.V. Sherstnev, Appl. Phys. Lett. 77 (2000) 872–874.
[3] X. Marcadet, A. Rakovska, I. Prevot, G. Glastre, B. Vinter, V. Berger, J. Cryst. Growth 227–228 (2001) 609–613.
[4] A. Rakovska, V. Berger, X. Marcadet, B. Vinter, G. Glastre, T. Oksenhendler, D. Kaplan, Appl. Phys. Lett. 77 (2000) 397–399.
[5] J.D. Kim, D. Wu, J. Wojkowski, J. Piotrowski, J. Xu, M. Razeghi, Appl. Phys. Lett. 68 (1996) 99–101.
[6] G.H. Avetisyan, V.B. Kulikov, V.P. Kotov, I.D. Zalevsky, P.V. Bulaev, A.A. Padalitza, SPIE 3200 (1996) 150–156.
[7] S. Nakamura, P. Jayavel, T. Koyama, M. Kumagawa, Y. Hayakawa, J. Cryst. Growth 280 (2005) 26–31.
[8] S. Nakamura, P. Jayavel, T. Koyama, Y. Hayakawa, J. Cryst. Growth 300 (2007) 497–502.
[9] R.M. Biefeld, C.R. Hills, S.R. Lee, J. Cryst. Growth 91 (1988) 515–526.
[10] H. Chen, L.W. Guo, Q. Cui, Q. Hu, Q. Huang, J.M. Zhou, J. Appl. Phys. 79 (1996) 1167–1169.
[11] C.F. Shih, N.C. Chen, S.Y. Lin, K.S. Liu, Appl. Phys. Lett. 86 (2005) 211103–211105.
[12] H. Yuan, S.J. Chua, Z. Miao, J. Dong, Y. Wang, J. Cryst. Growth 273 (2004) 63–67.
[13] I. Akasaki, J. Cryst. Growth 237–239 (2002) 905–911.
[14] S. Nakamura, P. Jayavel, T. Koyama, M. Kumagawa, Y. Hayakawa, J. Cryst. Growth 274 (2005) 362–366.
[15] Y.B. Li, S.S. Dosanjh, I.T. Ferguson, A.G. Norman, A.G. de. Ollveira, R.A. Stradling, R. Zallent, Semicond. Sci. Technol. 7 (1992) 567–570.
[16] Y.T. Cherng, K.Y. Ma, G.B. Stringfellow, Appl. Phys. Lett. 53 (1988) 886–887.
[17] K. Kakimoto, T. Katoda, Appl. Phys. Lett. 40 (1982) 826–828.
[18] S.D. Wu, L.W. Guo, Z.H. Li, X.Z. Shang, W.X. Wang, Q. Huang, J.M. Zhou, J. Cryst. Growth 277 (2005) 21–25.
[19] J.C. Lin, Y.K. Su, S.J. Chang, W.H. Lan, W.R. Chen, Y.C. Cheng, W.J. Lin, Y.C. Tzeng, H.Y. Shin, C.M. Chang, Opt. Mater., in press.
[20] R.J. Egan, V.W.L. Chin, T.L. Tansley, J. Appl. Phys. 75 (1994) 2473–2476.
[21] H.Y. Deng, X.K. Hong, W.Z. Fang, N. Dai, Mater. Charact. 58 (2007) 307–311.
[22] H.H. Wieder, A.R. Clawson, Thin Solid Film 15 (1973) 217–221.
[23] J. Shao, W. Lu, X. Lü, F.Y. Yue, Z.F. Li, S.L. Guo, J.H. Chu, Rev. Sci. Instrum. 77 (2006) 063104–063109.
[24] Z.M. Fang, K.Y. Ma, D.H. Jaw, R.M. Cohen, G.B. Stringfellow, J. Appl. Phys. 67 (1990) 7034–7039.